An efficient methodology based on 2.5D FEM-BEM for ground-borne vibration radiated by underground railway tunnels and the re-radiated noise emitted inside them

Doctoral Dissertation Presentation

Dhananjay Ghangale

Advisors:
Dr. Robert Arcos
Dr. Jordi Romeu

Overview

Introduction

Global outlook

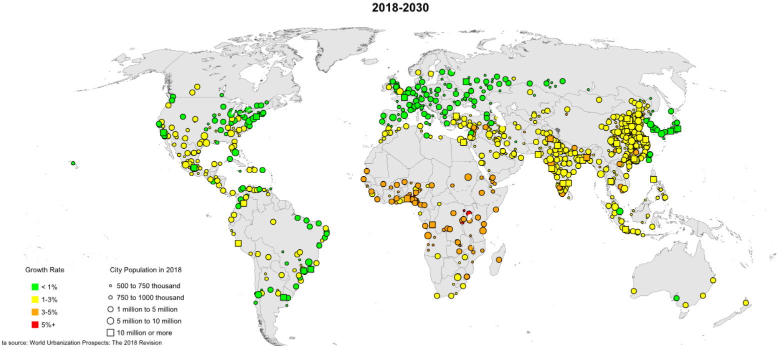

UNICEF

Global outlook

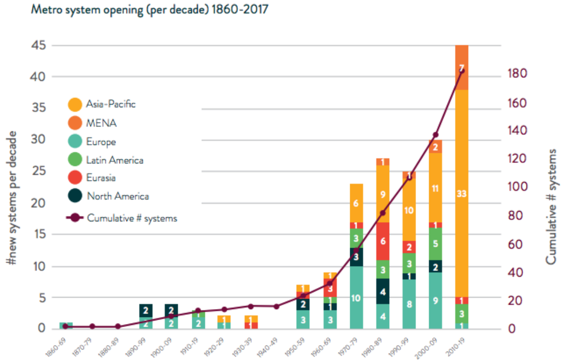

Total number of metro systems and the location of systems inaugurated each decade (bar).

UITP Observatory of Automated Metros

Global outlook

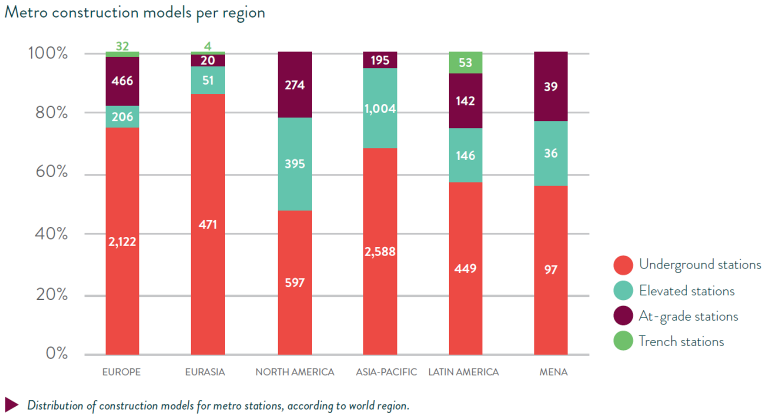

UITP Observatory of Automated Metros

Metro in News

mylondon (Europe-UK)
London family's nightmare as Tube trains make the walls rattle like thunder

Metro in News

mylondon (Europe-UK)
London family's nightmare as Tube trains make the walls rattle like thunder

NDTV (Asia-India)
Vibrations caused by Delhi Metro's underground trains creating cracks in buildings

Metro in News

mylondon (Europe-UK)
London family's nightmare as Tube trains make the walls rattle like thunder

NDTV (Asia-India)
Vibrations caused by Delhi Metro's underground trains creating cracks in buildings

Metro Reasons (America-USA)
A new Metro study confirms train vibrations, but has little recourse for residents

Justification of the work

- Models for SSI analysis:

Justification of the work

- Models for SSI analysis:
    1. Empirical

Justification of the work

- Models for SSI analysis:
  1. Empirical
  2. Semi-analytical

Justification of the work

- Models for SSI analysis:
    1. Empirical
    2. Semi-analytical
    3. Numerical

Justification of the work

Method	Modelling detail	Speed	Computational resources
Numerical	high	low	high
Semi-analytical	low	high	low

- Models for SSI analysis:
  1. Empirical
  2. Semi-analytical
  3. Numerical

Justification of the work

Method	Modelling detail	Speed	Computational resources
Numerical	high	low	high
Semi-analytical	low	high	low

- Models for SSI analysis:
  1. Empirical
  2. Semi-analytical
  3. Numerical

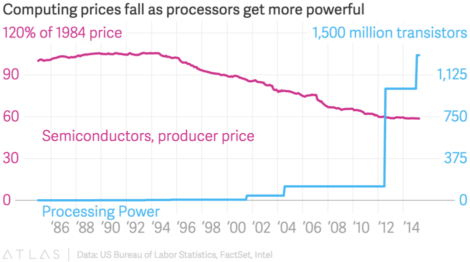

Justification of the work

Method	Modelling detail	Speed	Computational resources
Numerical	high	low	high
Semi-analytical	low	high	low

- Models for SSI analysis:
  1. Empirical
  2. Semi-analytical
  3. Numerical
     - 2D

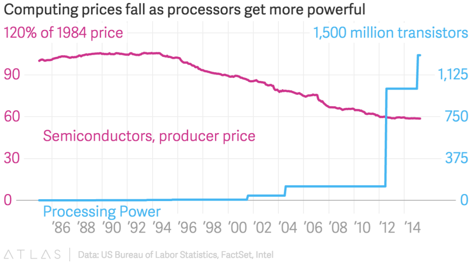

Justification of the work

Method	Modelling detail	Speed	Computational resources
Numerical	high	low	high
Semi-analytical	low	high	low

- Models for SSI analysis:
  1. Empirical
  2. Semi-analytical
  3. Numerical
     - 2D
     - 3D

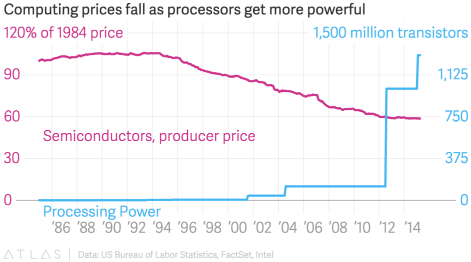

Justification of the work

Method	Modelling detail	Speed	Computational resources
Numerical	high	low	high
Semi-analytical	low	high	low

- Models for SSI analysis:
  1. Empirical
  2. Semi-analytical
  3. Numerical
     - 2D
     - 3D
     - 2.5D

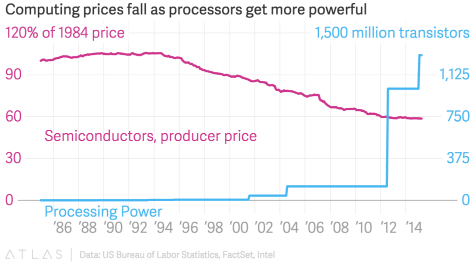

Thesis framework

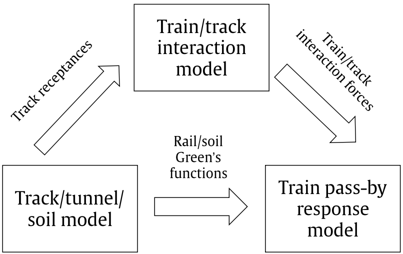

Thesis framework

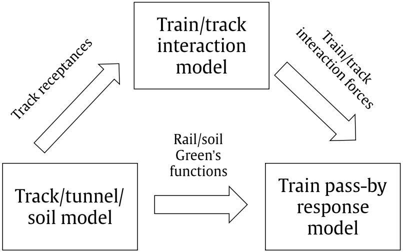

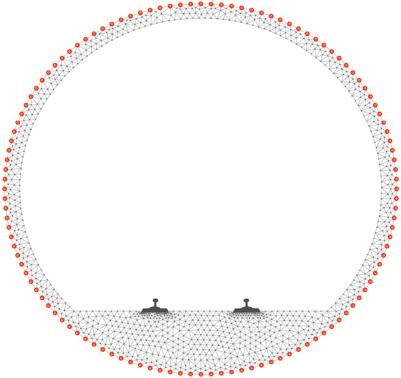

Thesis framework

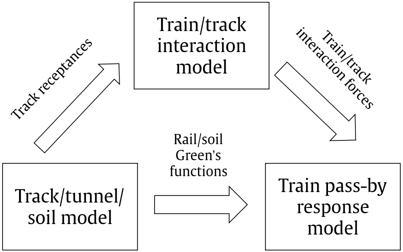

Track/tunnel/soil modelling

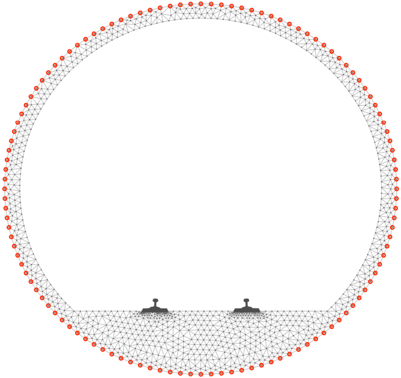

Thesis framework

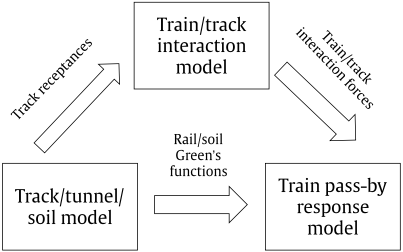

Track/tunnel/soil modelling

- 2.5D FEM-PML

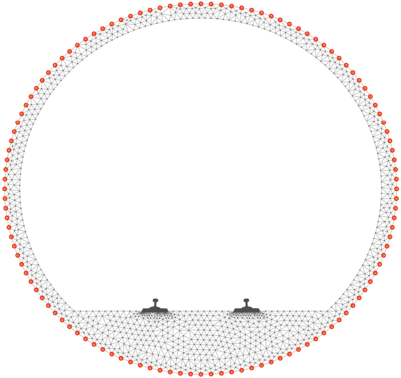

Thesis framework

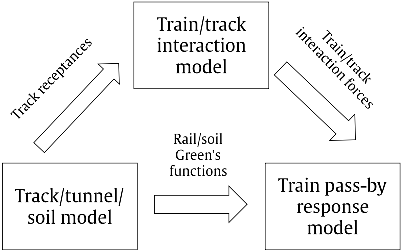

Track/tunnel/soil modelling

- 2.5D FEM-PML
- 2.5D FEM-MFS

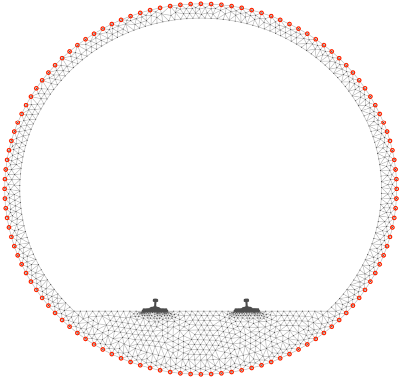

Thesis framework

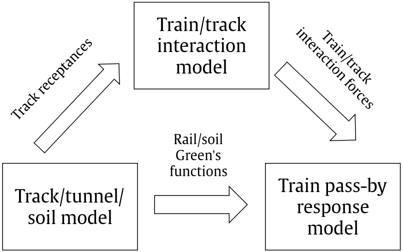

Track/tunnel/soil modelling

- 2.5D FEM-PML
- 2.5D FEM-MFS
- 2.5D FEM-BEM

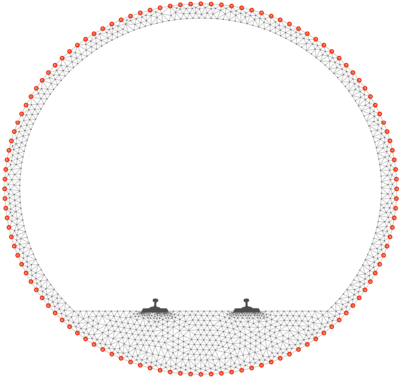

Thesis framework

Coupled elastodynamic FEM-BEM modelling approach based on 2.5D methodology.

*S. François et al. (2010), *M Bonnet (1995)

Thesis framework

Coupled elastodynamic FEM-BEM modelling approach based on 2.5D methodology.

1. 2.5D FEM-BEM based on globally regularised singular integrals.*

*S. François et al. (2010), *M Bonnet (1995)

Thesis framework

Coupled elastodynamic FEM-BEM modelling approach based on 2.5D methodology.

1. 2.5D FEM-BEM based on globally regularised singular integrals.*
2. Response is obtained by constructing a global stiffness matrix

$$[\mathsf{K}_0 - \mathrm{i}k_x\mathsf{K}_1 + k_x^2\mathsf{K}_2 + \bar{\mathsf{K}}_s - \omega^2\mathsf{M}]\bar{U} = \bar{F}.$$

*S. François et al. (2010), *M Bonnet (1995)

Thesis framework

Coupled elastodynamic FEM-BEM modelling approach based on 2.5D methodology.

1. 2.5D FEM-BEM based on globally regularised singular integrals.*
2. Response is obtained by constructing a global stiffness matrix

$$[\mathsf{K}_0 - \mathrm{i}k_x\mathsf{K}_1 + k_x^2\mathsf{K}_2 + \bar{\mathsf{K}}_s - \omega^2\mathsf{M}]\bar{U} = \bar{F}.$$

3. 2.5D FEM-BEM is extensively verified.

*S. François et al. (2010), *M Bonnet (1995)

Thesis framework

Coupled elastodynamic FEM-BEM modelling approach based on 2.5D methodology.

1. 2.5D FEM-BEM based on globally regularised singular integrals.*
2. Response is obtained by constructing a global stiffness matrix

$$[\mathsf{K}_0 - \mathrm{i}k_x\mathsf{K}_1 + k_x^2\mathsf{K}_2 + \bar{\mathsf{K}}_s - \omega^2\mathsf{M}]\bar{U} = \bar{F}.$$

3. 2.5D FEM-BEM is extensively verified.
4. Soil is modelled as full-space.

*S. François et al. (2010), *M Bonnet (1995)

Novelties proposed in 2.5D FEM-BEM

Order Complexity: $\mathcal{O}(n \log n)$

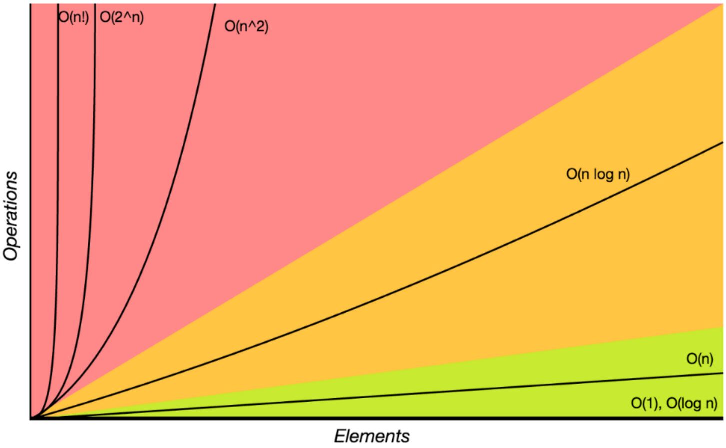

courtsey: bigocheatsheet.com

Fast Computation of Green's Function

- Computation time $\propto$ number of source/receiver points.

Fast Computation of Green's Function

- Computation time $\propto$ number of source/receiver points.
- Idea!!: Reduce number of source/receiver points.

Fast Computation of Green's Function

- Computation time $\propto$ number of source/receiver points.
- Idea!!: Reduce number of source/receiver points.

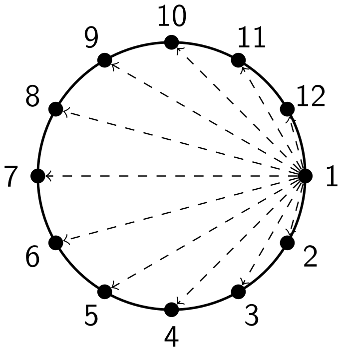

Fast Computation of Green's Function

- Computation time $\propto$ number of source/receiver points.
- Idea!!: Reduce number of source/receiver points.

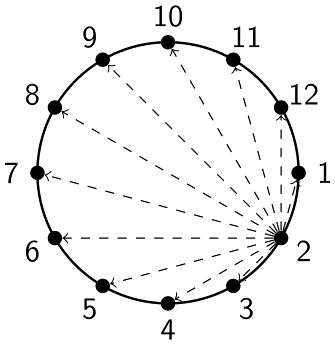

- Setting $z = 0$ in fullspace Green's functions allows: $F_G = f(\theta)f(r)$.

Fast Computation of Green's Function

- Computation time $\propto$ number of source/receiver points.
- Idea!!: Reduce number of source/receiver points.

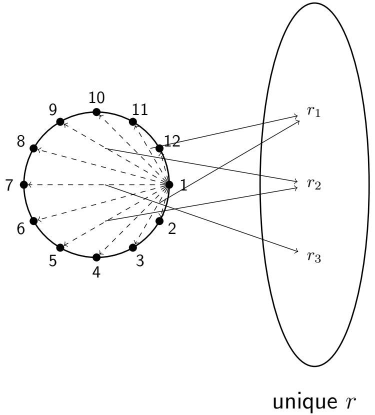

Fast Computation of Green's Function

- Computation time $\propto$ number of source/receiver points.
- Idea!!: Reduce number of source/receiver points.

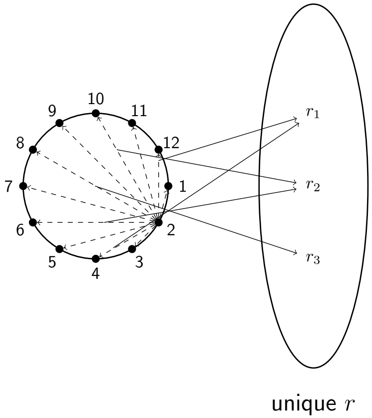

Fast Computation of Green's Function

- Computation time $\propto$ number of source/receiver points.
- Idea!!: Reduce number of source/receiver points.

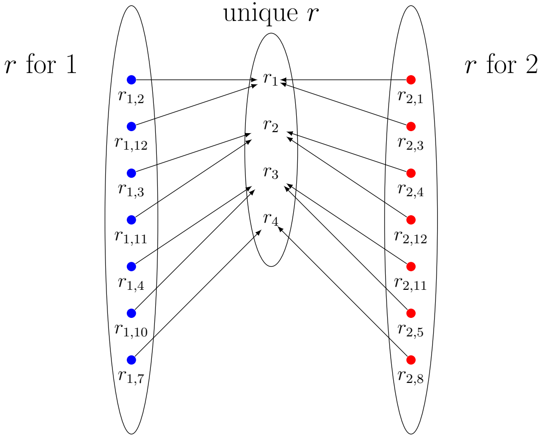

- $r \xrightarrow{unique} r_u$ compute: $Fg\ \forall\ r_u$ then construct: $F_G = f(\theta)\mathcal{M}(F_g)$.

Fast Computation of Green's Function

- Computation time $\propto$ number of source/receiver points.
- Idea!!: Reduce number of source/receiver points.
- Green's displacements:

$$\bar{\mathsf{H}} = \mathsf{T}_\theta^{-1}\mathcal{M}(\bar{\mathsf{H}}_{us})\mathsf{T}_\theta$$

- Green's tractions:

$$\bar{\mathsf{T}} = \mathsf{T}_\theta^{-1}(\mathcal{M}(\bar{\mathsf{T}}_{us}) \circ \mathsf{T}_\phi)\mathsf{T}_\theta.$$

Axisymmetric Formulation

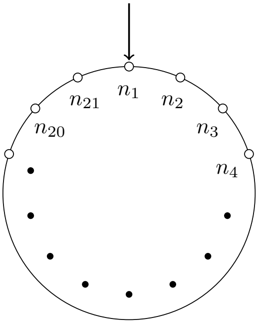

$\mathsf{G}_{i,j}$ $(i = 1)$

Axisymmetric Formulation

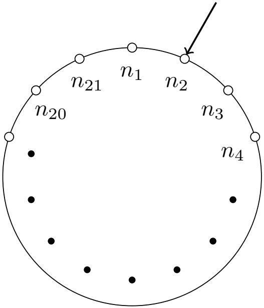

$\mathsf{G}_{i,j}$ $(i = 2)$

Axisymmetric Formulation

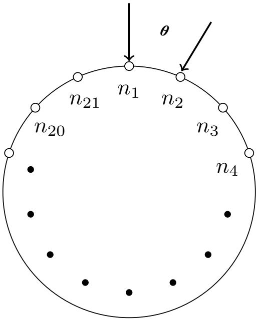

$\mathsf{G}_{2,j} \simeq \mathsf{G}_{1,j}$ except for relative rotation between $i = 1$ and $i = 2$.

Axisymmetric Formulation

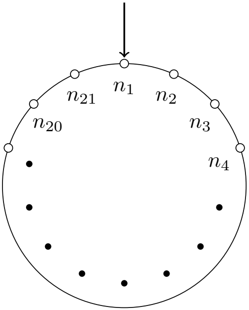

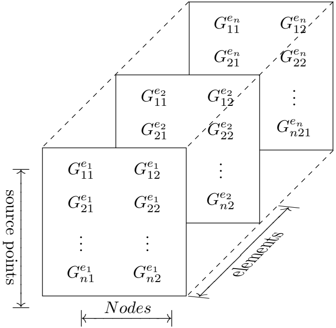

$$\mathsf{G}_{i,j}\ (\forall i \in \{2, n\}) = \mathcal{M}(\mathsf{T}^{-1}_{\theta_{rel}} \mathsf{G}_{1,j} \mathsf{T}_{\theta_{rel}})$$

Accurate modelling of train response

Train/track interaction

- Two components of the loads are considered:

Train/track interaction

- Two components of the loads are considered:
  1. Quasi static load
  2. Dynamic load

Train/track interaction

- Two components of the loads are considered:
  1. Quasi static load
  2. Dynamic load
- Wheel/rail contact is modelled with linear Hertz contact theory.

Train/track interaction

- Two components of the loads are considered:
    1. Quasi static load
    2. Dynamic load
- Wheel/rail contact is modelled with linear Hertz contact theory.
- Wheel/rail dynamic loads are given by:

$$F^{w/r} = \left(\mathrm{H}_v^{w/r} + \mathrm{H}_r^{w/r} + k_H^{-1}\mathrm{I}\right)^{-1} E_r.$$

Train/track interaction

- Two components of the loads are considered:
  1. Quasi static load
  2. Dynamic load
- Wheel/rail contact is modelled with linear Hertz contact theory.
- Wheel/rail dynamic loads are given by:

$$F^{w/r} = \left(\mathsf{H}_v^{w/r} + \mathsf{H}_r^{w/r} + k_H^{-1}\mathsf{I}\right)^{-1} E_r.$$

- Displacement obtained after train pass:

$$u(\tilde{x}, t) = \frac{1}{4\pi^2} \int_{-\infty}^{+\infty} \sum_{n=1}^{N_a} \left[\int_{-\infty}^{+\infty} \tilde{H}_s^r F_n^{w/r} \mathrm{e}^{-\mathrm{i}k_x(\tilde{x}-\tilde{x}_n)} \mathrm{d}k_x \right] \mathrm{e}^{\mathrm{i}\tilde{\omega}t} \mathrm{d}\tilde{\omega}.$$

Wavenumber-frequency sampling

- 3D response of train pass-by $\propto$ the Green's functions of the system sampled in 2.5D.

Wavenumber-frequency sampling

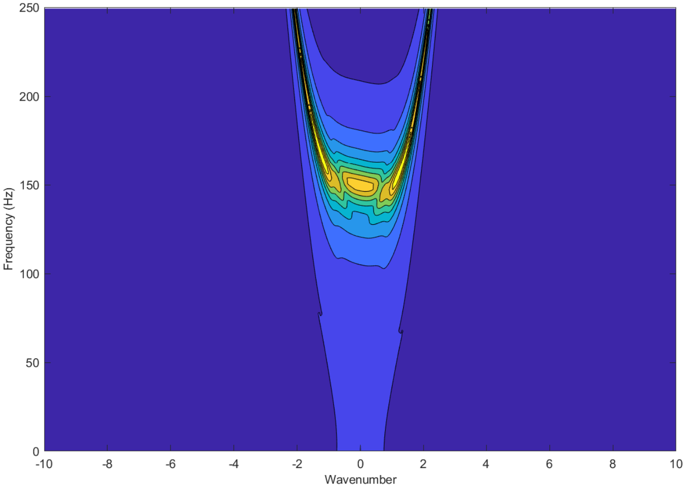

Wavenumber-frequency sampling

- To accurately compute the train pass-by in 2.5D a sampling strategy:
  1. Linear on moving frequency.
  2. Non-uniform on wavenumber which varies with frequency.

Frequency sampling

ω_{max} , N_ω

Compute:
$\tilde{\omega}_{max} = \omega_{max}(1 + v_t/C_{min})$

Compute:
$\text{linspace}(0, \tilde{\omega}_{max}, N_\omega)$

Sampling vector of $\tilde{\omega}$

Wavenumber presampling

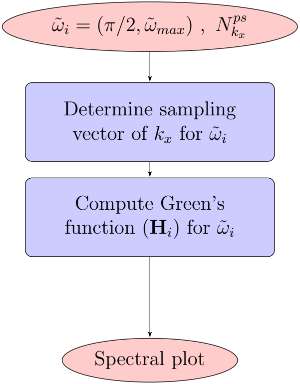

Wavenumber presampling

Determining the pre-sampling vector of k_x for $\tilde{\omega}_i$:

- Compute limits for k_x as:

$$k_{x_i}^{\mathrm{lim}} = \tilde{\omega}/c_i \; \forall \; N_{ss}$$

- Presampling k_x vector:

$$\mathrm{linspace}(-2k_{xi}^{\mathrm{lim}},\; 2k_{xi}^{\mathrm{lim}},\; (N_{k_x}^{ps}/2N_{ss}))$$

$$\pm\mathrm{logspace}(2k_{xi}^{\mathrm{lim}},\; 10^5, (N_{k_x}^{ps}/4N_{ss}))$$

Wavenumber presampling

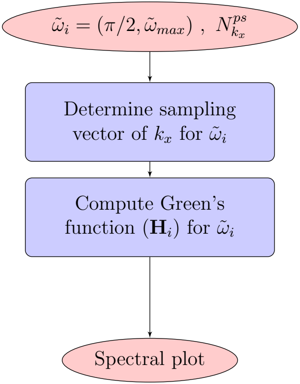

Wavenumber sampling

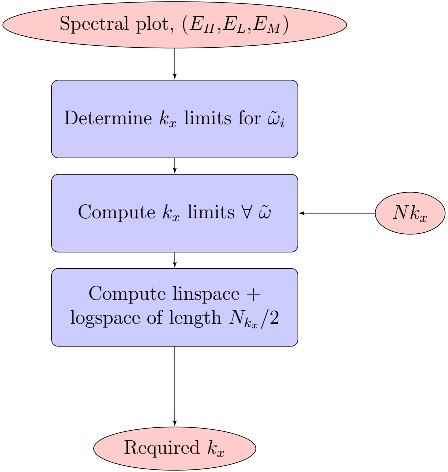

Wavenumber sampling

Determining the wavenumber limits for $\tilde{\omega}_i$:

- 10% tolerance for linear sampling $\implies$ 90% spectral content of Green's function.
- 1% tolerance for logarithmic sampling $\implies$ 90 $\rightarrow$ 99% spectral content of Green's function.

Wavenumber sampling

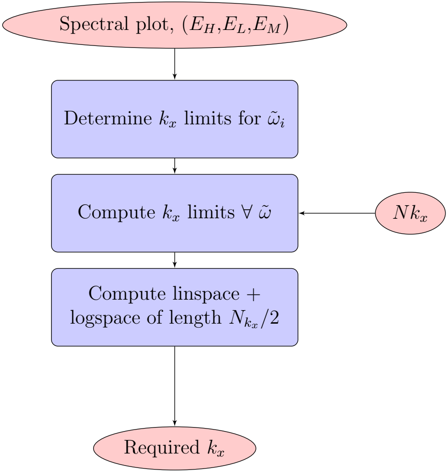

Wavenumber sampling

Determining the wavenumber limits for all $\tilde{\omega}$:

- Wavenumber limits vary linearly with frequency

$$k_{x_{\mathrm{lin}}}^{\mathrm{lim}}(\tilde{\omega}) = \left(\frac{\tilde{\omega} - \pi/2}{\tilde{\omega}_{\mathrm{max}} - \pi/2}\right)\left(k_{x_{\mathrm{lin}}}^{\mathrm{lim}_u} - k_{x_{\mathrm{lin}}}^{\mathrm{lim}_d}\right) + k_{x_{\mathrm{lin}}}^{\mathrm{lim}_u}$$

and

$$k_{x_{\mathrm{log}}}^{\mathrm{lim}}(\tilde{\omega}) = \left(\frac{\tilde{\omega} - \pi/2}{\tilde{\omega}_{\mathrm{max}} - \pi/2}\right)\left(k_{x_{\mathrm{log}}}^{\mathrm{lim}_u} - k_{x_{\mathrm{log}}}^{\mathrm{lim}_d}\right) + k_{x_{\mathrm{log}}}^{\mathrm{lim}_u}$$

Wavenumber sampling

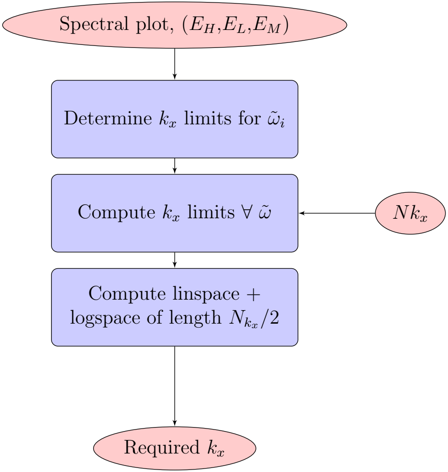

Vibration energy flow

Vibration Energy-Flow

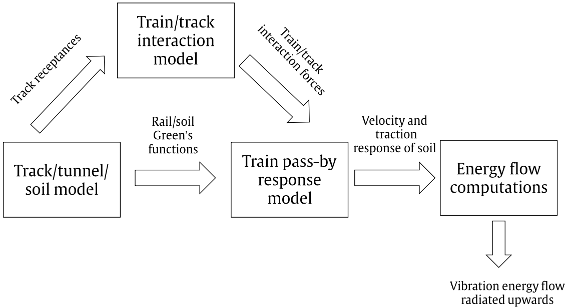

Model for the vibration propagation in the soil

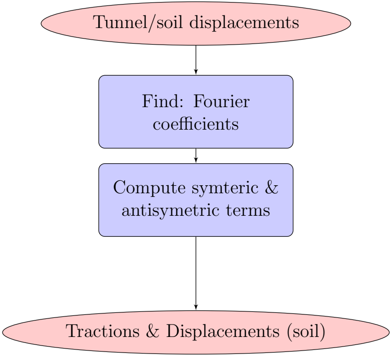

Model for the vibration propagation in the soil

From the displacement in tunnel/soil interface unknown Fourier Coefficients $\bar{C}^i_n$, $(i = s/a)$ are found by inverting:

$$\bar{U}^i_n(r_b) = \bar{\mathrm{U}}^i_{cn}(r_b)\bar{C}^i_n.$$

Forrest and Hunt et al. (2006), Clot (2014)

Model for the vibration propagation in the soil

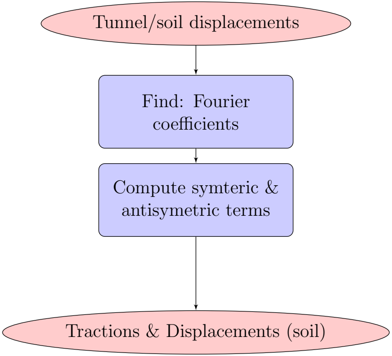

Model for the vibration propagation in the soil

After which the symmetric and anti-symmetric terms for any radial location in soil r_f are found

$$\bar{U}_n^i(r_f) = \bar{\mathsf{U}}_{cn}^i(r_f)\bar{C}_n^i,$$

and

$$\bar{T}_n^i(r_f) = \bar{\mathsf{T}}_{cn}^i(r_f)\bar{C}_n^i.$$

The displacements and tractions in soil at any radial location in soil r_f are given by

$$\bar{U}_s(r_f,\theta) = \sum_{n=0}^{\infty}[\mathsf{S}_n^s(\theta)\bar{U}_n^s(r_f) + \mathsf{S}_n^a(\theta)\bar{U}_n^a(r_f)].$$

and

$$\bar{T}_s(r_f,\theta) = \sum_{n=0}^{\infty}[\mathsf{S}_n^s(\theta)\bar{T}_n^s(r_f) + \mathsf{S}_n^a(\theta)\bar{T}_n^a(r_f)].$$

Forrest and Hunt et al. (2006), Clot (2014)

Vibration energy flow

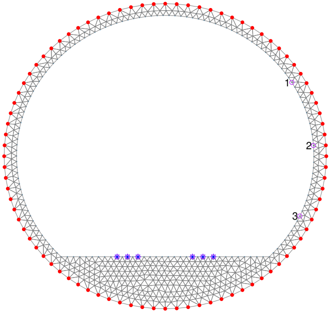

DFF (grey)

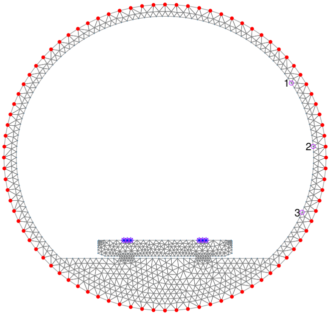

FST (black)

Vibration energy flow

Two types of soil are considered:

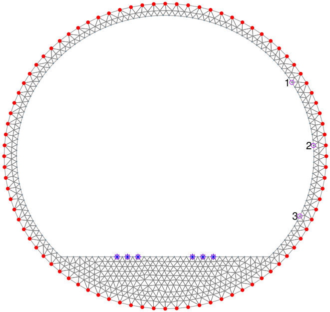

DFF (grey)

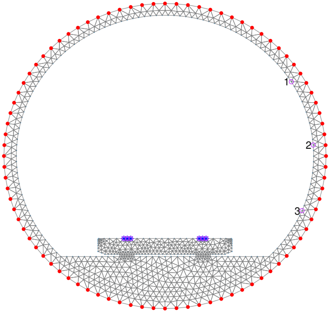

FST (black)

Vibration energy flow

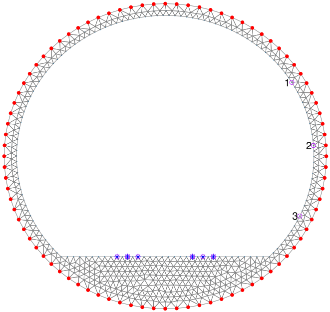

DFF (grey)

Two types of soil are considered:

- Soft Soil (b) ($E = 180$ MPa).
- Hard Soil (a) ($E = 480$ MPa).

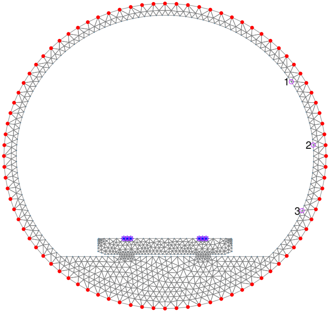

FST (black)

Vibration energy flow

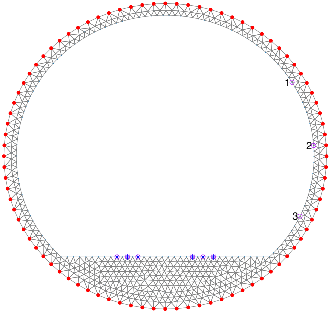

DFF (grey)

Two types of soil are considered:

- Soft Soil (b) ($E = 180$ MPa).
- Hard Soil (a) ($E = 480$ MPa).
- 38 evaluators in soil at a specific r.

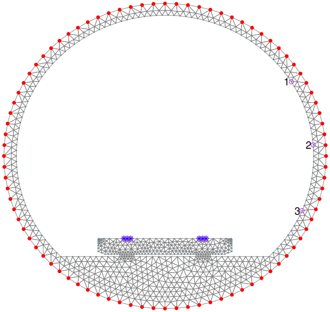

FST (black)

Vibration energy flow

- Energy flow:

$$E = \int_{-\infty}^{\infty} P(t)\mathrm{d}t,$$

- Power flow is defined as:

$$P(t) = \int_S \boldsymbol{v}(\boldsymbol{x}, t)\cdot\boldsymbol{\tau}(\boldsymbol{x}, t)\mathrm{d}S,$$

Vibration energy flow

- Energy flow:

$$E = \int_{-\infty}^{\infty} P(t)\mathrm{d}t,$$

- Power flow is defined as:

$$P(t) = \int_S \boldsymbol{v}(\boldsymbol{x}, t)\cdot\boldsymbol{\tau}(\boldsymbol{x}, t)\mathrm{d}S,$$

- Vibration energy flow radiated upwards in soft soil

Track type	5 m	15 m
DFF	0.2547 J/m	0.1691 J/m
FST	0.2227 J/m	0.1711 J/m

Vibration energy flow

- Energy flow:

$$E = \int_{-\infty}^{\infty} P(t)\mathrm{d}t,$$

- Power flow is defined as:

$$P(t) = \int_S \boldsymbol{v}(\boldsymbol{x}, t)\cdot\boldsymbol{\tau}(\boldsymbol{x}, t)\mathrm{d}S,$$

- Vibration energy flow radiated upwards in soft soil

Track type	5 m	15 m
DFF	0.2547 J/m	0.1691 J/m
FST	0.2227 J/m	0.1711 J/m

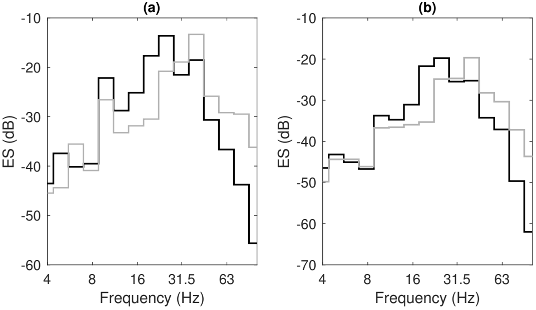

- (a) 5 m (b) 15 m
- DFF (grey) FST (black)

Vibration energy flow

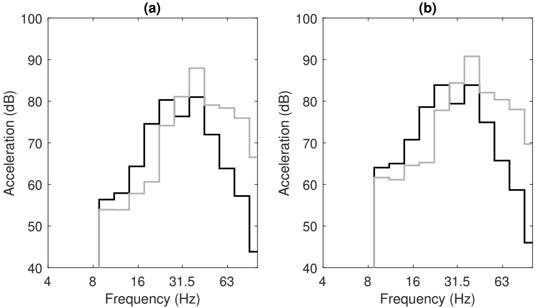

- DFF (grey) FST (black)
- Hard soil (a) Soft Soil (b)

Vibration energy flow

- FST is better at reducing vibration at higher frequencies.

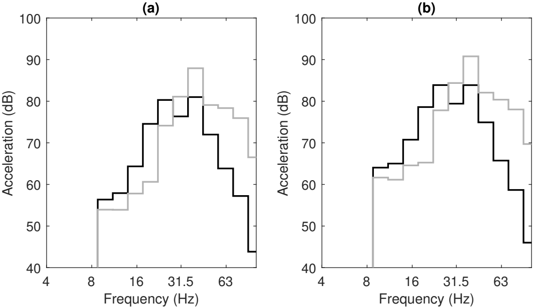

- DFF (grey) FST (black)
- Hard soil (a) Soft Soil (b)

Vibration energy flow

- FST is better at reducing vibration at higher frequencies.
- Level of vibration in soft soil > hard soil.

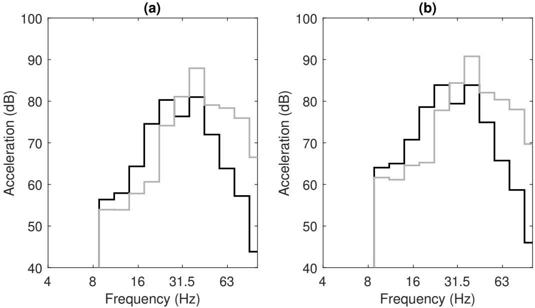

- DFF (grey) FST (black)
- Hard soil (a) Soft Soil (b)

Vibration energy flow

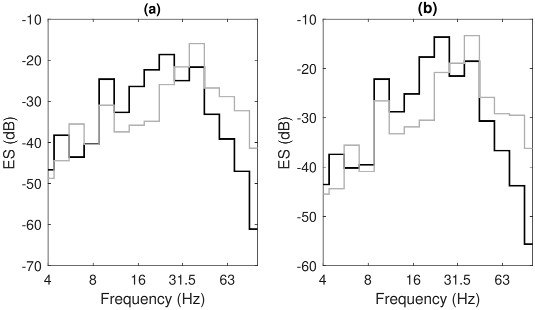

- DFF (grey) FST (black)
- Hard soil (a) Soft Soil (b)

Vibration energy flow

- FST shifts the energy spectra to lower frequencies.

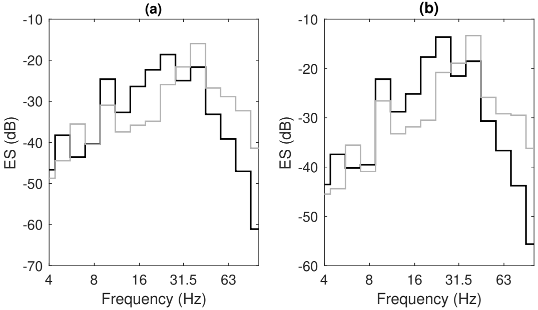

- DFF (grey) FST (black)
- Hard soil (a) Soft Soil (b)

Vibration energy flow

- FST shifts the energy spectra to lower frequencies.
- Local soil affects in levels of induced vibrations and vibration energy radiated.

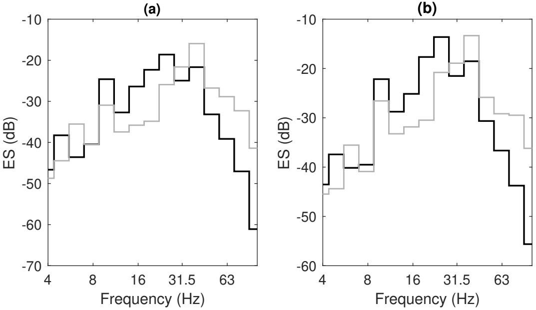

- DFF (grey) FST (black)
- Hard soil (a) Soft Soil (b)

Validity of using one accelerometer

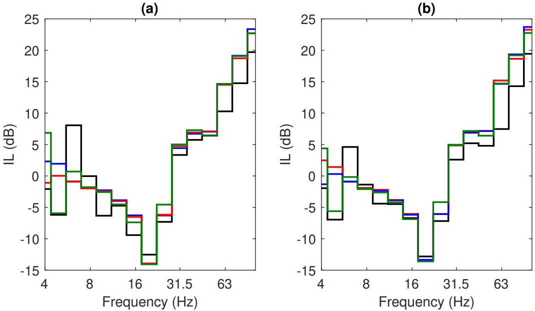

- ESD (black) accleration (colored)
- Hard soil (a) Soft Soil (b)

- Insertion loss by energy spectral density:

$$\mathrm{IL_{ES}} = 10\log_{10}\left(\frac{\mathrm{ES_{FST}}}{\mathrm{ES_{DFF}}}\right);$$

- Insertion loss by acceleration:

$$\mathrm{IL_a} = 20\log_{10}\left(\frac{a_{\mathrm{FST}}}{a_{\mathrm{DFF}}}\right).$$

Validity of using one accelerometer

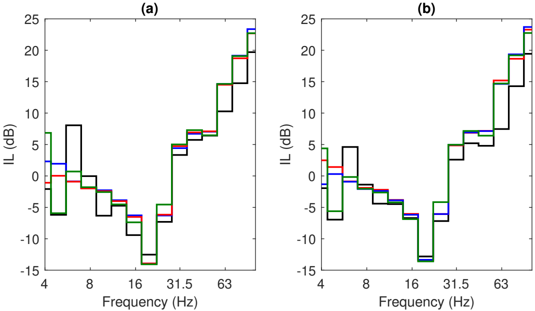

- ESD (black) accleration (colored)
- Hard soil (a) Soft Soil (b)

- Insertion loss by energy spectral density:

$$\mathrm{IL_{ES}} = 10\log_{10}\left(\frac{\mathrm{ES_{FST}}}{\mathrm{ES_{DFF}}}\right);$$

- Insertion loss by acceleration:

$$\mathrm{IL_{a}} = 20\log_{10}\left(\frac{a_{\mathrm{FST}}}{a_{\mathrm{DFF}}}\right).$$

- $\mathrm{IL_a} \simeq \mathrm{IL_{ES}}$.

Validity of using one accelerometer

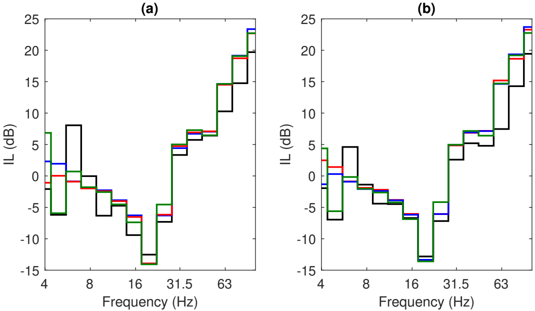

- ESD (black) accleration (colored)
- Hard soil (a) Soft Soil (b)

- Insertion loss by energy spectral density:

$$\mathrm{IL_{ES}} = 10\log_{10}\left(\frac{\mathrm{ES_{FST}}}{\mathrm{ES_{DFF}}}\right);$$

- Insertion loss by acceleration:

$$\mathrm{IL_{a}} = 20\log_{10}\left(\frac{a_{\mathrm{FST}}}{a_{\mathrm{DFF}}}\right).$$

- $\mathrm{IL_a} \simeq \mathrm{IL_{ES}}$.
- Mismatch at high & low frequencies of about 8 dB.

Validity of using one accelerometer

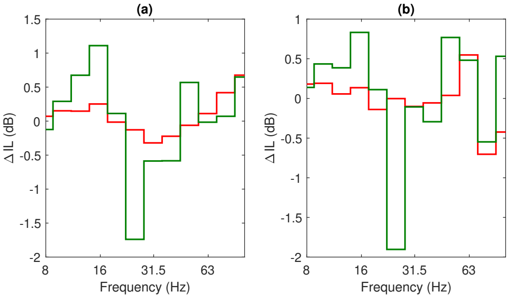

- Hard soil (a) Soft Soil (b)

Validity of using one accelerometer

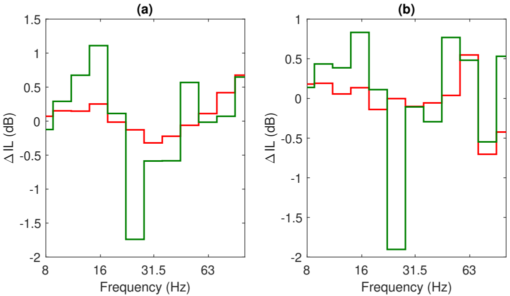

- Hard soil (a) Soft Soil (b)

- IL of a mitigation measure could be significantly dependent on the local subsoil surrounding.

Validity of using one accelerometer

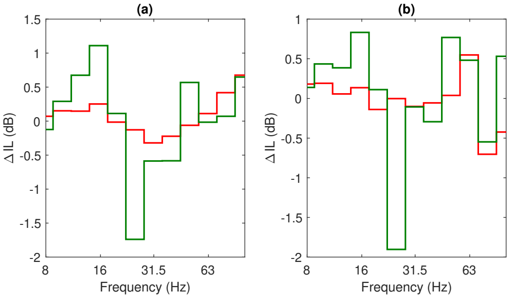

- Hard soil (a) Soft Soil (b)

- IL of a mitigation measure could be significantly dependent on the local subsoil surrounding.
- Variations in the IL associated with the vibration acceleration are found to be small $\Longrightarrow$ location of the accelerometer is not of great importance.

Re-radiated noise

Re-radiated Noise

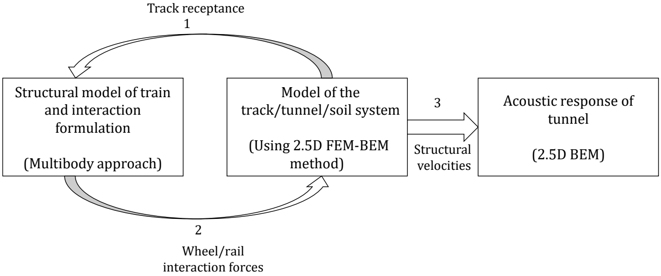

Ghangale et al. (2019)

2.5D Acoustic BEM

- Global regularisation is extended to 2.5D Acoustic BEM.
- Two step procedure:
    1. Solve BIE to find boundary unknowns:

$$\bar{\mathsf{H}}_b \bar{P}_{n_b} = \mathrm{i}\rho\omega \bar{\mathsf{G}}_b \bar{V}_{n_b}.$$

    2. Then find pressure in domain:

$$\bar{P}_{n_f} = -(\bar{\mathsf{H}}_f \bar{P}_{n_b} + \mathrm{i}\rho\omega \bar{\mathsf{G}}_f \bar{V}_{n_b}).$$

Ghangale et al. (2019)

2.5D Acoustic BEM

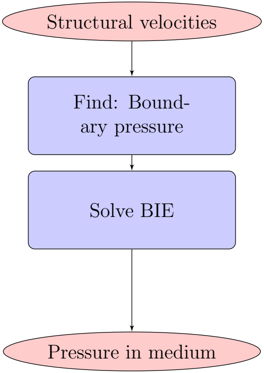

Decoupled approach.

Colaço et al. (2017)

Vibration and re-radiated noise inside underground tunnels

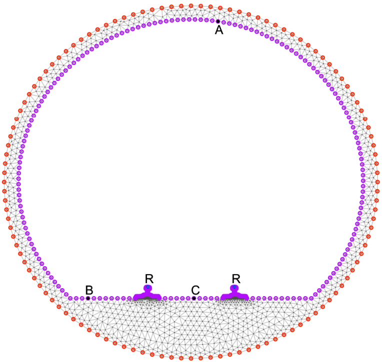

Vibration and re-radiated noise inside underground tunnels

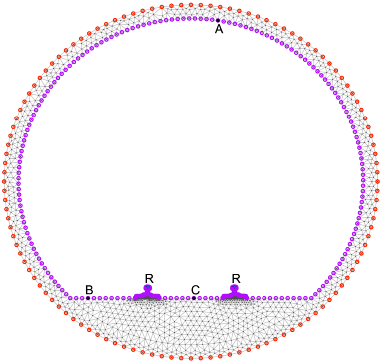

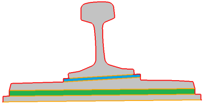

Vibration and re-radiated noise inside underground tunnels

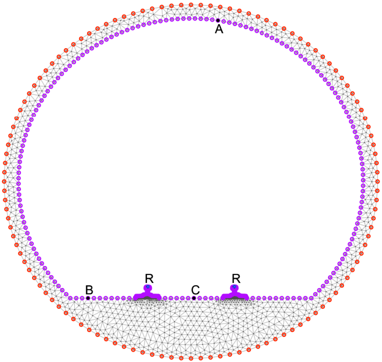

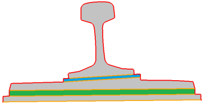

- Case 1: Stiffer rail pad (black) ($E_t = 1.15$ MPa), ($E_b = 2.7$ MPa)

Vibration and re-radiated noise inside underground tunnels

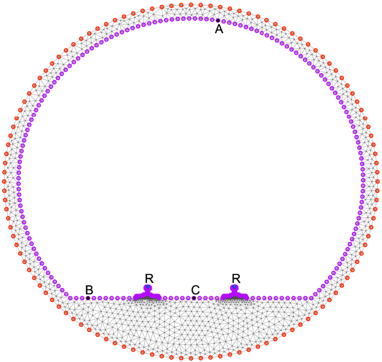

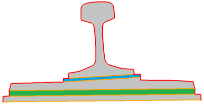

- Case 1: Stiffer rail pad (black) $(E_t = 1.15\ \mathrm{MPa})$, $(E_b = 2.7\ \mathrm{MPa})$
- Case 2: Softer rail pad (grey) $(E_t = 0.3\ \mathrm{MPa})$, $(E_b = 0.7\ \mathrm{MPa})$

Vibration and re-radiated noise inside underground tunnels

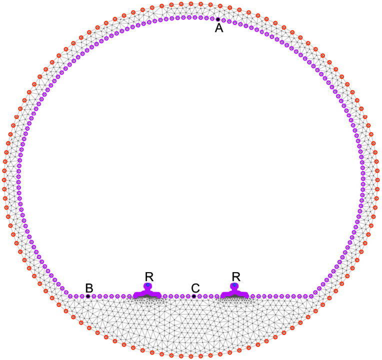

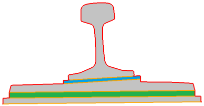

- Case 1: Stiffer rail pad (black) ($E_t = 1.15$ MPa), ($E_b = 2.7$ MPa)
- Case 2: Softer rail pad (grey) ($E_t = 0.3$ MPa), ($E_b = 0.7$ MPa)
- Case 3: No rail pads (dashed)

Influence of fastener stiffness on vibrations inside underground tunnels

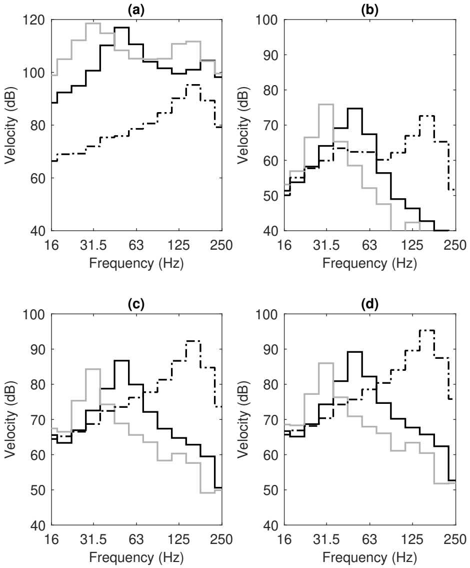

Influence of fastener stiffness on vibrations inside underground tunnels

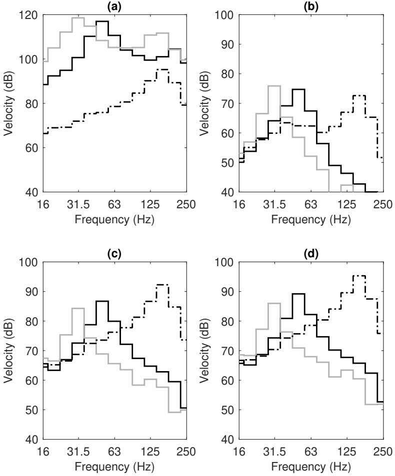

- rail response (a) tunnel response (b,c,d)

- Stiffer rail pads $\Longrightarrow$ shifts vibration radiation to higher frequencies.
- Softer rail pads $\Longrightarrow$ more rail vibration and less vibration from tunnel.
- No rail pads $\Longrightarrow$ rail and tunnel structure have identical vibration radiation.

Influence of fastener stiffness on re-radiated noise inside underground tunnels

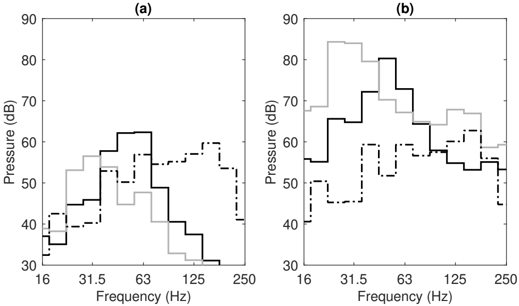

- case 1 (black) case 2 (grey) case 3 (dashed)
- noise levels by tunnel (a)
  noise levels by rail + tunnel (b)

Influence of fastener stiffness on re-radiated noise inside underground tunnels

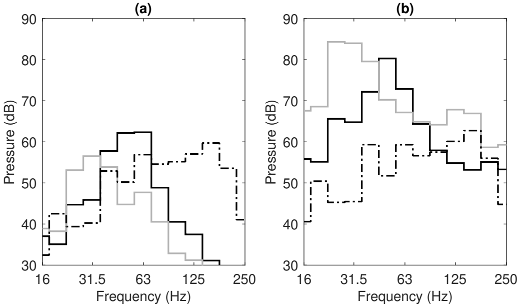

- Total noise pressure level is influenced by rails.

- case 1 (black) case 2 (grey) case 3 (dashed)
- noise levels by tunnel (a)
  noise levels by rail + tunnel (b)

Influence of fastener stiffness on re-radiated noise inside underground tunnels

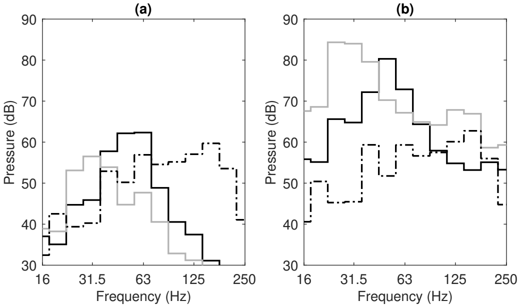

- case 1 (black) case 2 (grey) case 3 (dashed)
- noise levels by tunnel (a)
  noise levels by rail + tunnel (b)

- Total noise pressure level is influenced by rails.
- Softer fastener increases total noise pressure levels inside the tunnel.

Conclusions

Summary

1. 2.5D FEM-BEM for elastodynamics
   - Fast Computation of Green's functions.
   - Axisymmetric approach for underground tunnel.
2. 2.5D BEM for acoustics based on globally regularised integrals.
3. Methodology for computing vibration energy flow by underground railway infrastructures.
4. Methodology for computing re-radiated noise.
5. New non-uniform wavenumber sampling for train response.

Summary

Conclusion from vibration energy flow study:

Summary

Conclusion from vibration energy flow study:

1. FST is reducing drastically the levels of vibration as compared with the DFF system at higher frequencies.
2. FST shifts the vibration spectrum to lower frequencies.
3. The shift on frequency spectrum observed in FST does not imply a change on the energy radiated.

Summary

Conclusion from preliminary study of validity of using once accelerometer:

Summary

Conclusion from preliminary study of validity of using once accelerometer:

1. Difference of 8dB were found between $\mathrm{IL_a}$ & $\mathrm{IL_{ES}}$. .
2. Variations in the IL associated with the vibration acceleration are found to be small $\implies$ location of the accelerometer is not of great importance.
3. More parametric studies are required to accurately determine the validity of using one accelerometers for assessing a vibration reducing countermeasure.

Summary

Conclusion from re-radiated noise study:

Summary

Conclusion from re-radiated noise study:

1. Softer fastener shifts vibration spectra to low frequencies.
2. Softer fastener is a more efficient solution for vibration mitigation as it decrease vibration level of tunnel structures.
3. Noise levels in tunnels is influenced by rails noise radiation when vehicle is not considered.
4. Noise levels in the tunnel increases when rail vibration increases.

Publications

A methodology based on structural FEM-BEM and acoustic BEM models in 2.5D for the prediction of re-radiated noise in railway-induced ground-borne vibration problems

Journal of Vibration and Acoustics, 2019 (3)

Dhananjay Ghangale, Aires Colaço, Pedro Alves Costa, Robert Arcos

Publications

A methodology based on structural FEM-BEM and acoustic BEM models in 2.5D for the prediction of re-radiated noise in railway-induced ground-borne vibration problems
Journal of Vibration and Acoustics, 2019 (3)
Dhananjay Ghangale, Aires Colaço, Pedro Alves Costa, Robert Arcos

A methodology based on 2.5D FEM-BEM for the evaluation of the vibration energy flow radiated by underground railway infrastructures
Journal of Computer Methods in Applied Mechanics and Engineering, (submitted)
Dhananjay Ghangale, Robert Arcos, Arnau Clot, Julen Cayero, Jordi Romeu

Publications

A methodology based on structural FEM-BEM and acoustic BEM models in 2.5D for the prediction of re-radiated noise in railway-induced ground-borne vibration problems
Journal of Vibration and Acoustics, 2019 (3)
Dhananjay Ghangale, Aires Colaço, Pedro Alves Costa, Robert Arcos

A methodology based on 2.5D FEM-BEM for the evaluation of the vibration energy flow radiated by underground railway infrastructures
Journal of Computer Methods in Applied Mechanics and Engineering, (submitted)
Dhananjay Ghangale, Robert Arcos, Arnau Clot, Julen Cayero, Jordi Romeu

Study of validity of using one accelerometer for assessing the efficiency of vibration reducing countermeasures
Journal of Tunnelling and Underground Space Technology, (in process)
Dhananjay Ghangale, Robert Arcos, Arnau Clot, Jordi Romeu

Future Work

Modelling the complete train/track/structure/soil/building system

- Fast half-space solutions.
- Publication on track/soil coupling load.

Developing Fast Solvers

- MFS.
- SBM.
- General energy flow computation.

Hybrid Methodology

- For assessing the vibration reducing countermeasure where track already exist.
- Experimental measurements + numerical modelling.

¡Thank you for your attention!